



Sharif University of Technology

Scientia Iranica

Transactions B: Mechanical Engineering

www.sciencedirect.com

Effects of gas properties and geometrical parameters on performance of a vortex tube

H. Khazaei^{a,*}, A.R. Teymourtash^a, M. Malek-Jafarian^b

^a Ferdowsi University of Mashhad, Mashhad, P.O. Box 91735-134, Iran

^b Birjand University, Birjand, P.O. Box 97175-615, Iran

Received 4 July 2011; revised 6 October 2011; accepted 3 March 2012

KEYWORDS

Vortex tube;
Numerical method;
Standard *k*-epsilon;
Spalart–Allmaras;
RSM;
Different gases.

Abstract In this paper, energy separation effects in a vortex tube have been investigated using a CFD model. A numerical simulation has been undertaken, due to the complex structure of flow. The governing equations have been solved by the FLUENT™ code in a 2D compressible and turbulent model. Three turbulent models, namely, RSM, Standard *k*-epsilon and Spalart–Allmaras, have been used. The Spalart–Allmaras turbulent model, which is the first equation, was not so bad in predicting temperature results, although the Standard *k*-epsilon model better predicts the results in most regions. The effects of geometrical parameters have been investigated. The results have shown that the hot outlet size and its shape do not affect the energy distribution in the vortex tube, and a very small diameter will decrease the temperature separation. Different kinds of gas have been examined for the vortex tube, and it was concluded that using helium as a refrigerant produces the largest energy separation.

© 2012 Sharif University of Technology. Production and hosting by Elsevier B.V.

Open access under [CC BY-NC-ND license](http://creativecommons.org/licenses/by-nc-nd/4.0/).

1. Introduction

In recent decades, swirling flows have become an interesting research topic, due to their various industrial applications. A vortex tube is one whose operation is based on the existence of swirling flow. In this equipment, air (i.e. operating gas), at high pressure, enters the main tube tangentially via a few nozzles and divides into two spiral and low pressure flows, with higher and lower temperatures than the inlet temperature. This phenomenon, i.e. the dividing of flow into two temperature areas, is known as an energy separation effect. The schematic diagram of the vortex tube has been shown in Figure 1 [1].

Vortex tubes have widely been used in various applications where compactness, safety and low equipment cost are basic factors, including heating and cooling applications, gas

liquefaction, separation of gas mixtures, drying of gases, uses in the chemical industry, electricity production, and snow making etc.

Even though the Ranque–Hilsch vortex tube effect has been the subject of numerous theoretical and experimental studies [2,3], no indisputable physical explanation of its effect has been found to this day.

Kurosaka invoked an acoustic streaming process. Stephan et al. proposed Gortler vortices as the main transfer mechanism. Amitani et al. explained it in view of the compressibility of the working fluid [3].

Balmer [4], who investigated, theoretically, the temperature separation phenomenon in a vortex tube, used the second law of thermodynamics to show that the temperature separation effect with a net increase in entropy is possible when incompressible liquids are used in the tube. This was confirmed by experiments with liquid water, which showed that temperature separation occurs when an inlet pressure is sufficiently high.

In a vortex tube, the temperature of a cold stream drop or temperature reduction is defined as the difference in temperature between that of an inlet stream and that of a cold stream:

$$\Delta T_c = T_i - T_c, \quad (1)$$

in which T_i is the temperature of the inlet stream and T_c is the temperature of a cold stream.

* Corresponding author. Tel.: +98 915 3256467.

E-mail addresses: Hosseinkhazaei1365@yahoo.com (H. Khazaei), Teymourtash@um.ac.ir (A.R. Teymourtash), mmjafarian@excite.com (M. Malek-Jafarian).

Peer review under responsibility of Sharif University of Technology.



Production and hosting by Elsevier

Nomenclature

D	Vortex tube diameter (m)
c_p	Specific heat at constant pressure (kJ/kg k)
COP	Coefficient of performance
T	Temperature (K)
ΔT	Temperature drop (K)
\tilde{v}	Transported variable in the Spalart–Allmaras model
k	Turbulent kinetic energy
ε	Dissipation rate of kinetic energy
T_t	Total temperature (K)
T_s	Static temperature (K)
V	Velocity magnitude (m/s)
P_0	Total pressure (Pa)
P_s	Static pressure (Pa)
M	Mach No.

Similarly, hot temperature differences are defined as:

$$\Delta T_h = T_h - T_i. \quad (2)$$

Most experiments provide inlet data, such as pressure, P_i , temperature, T_i , and mass flow rate just before the nozzle. Unfortunately, they cannot be used as input data for computations which need the data at the nozzle exit stage. Little is known about static pressure, temperature, T_i , and velocity at the nozzle outlet. Those values may be obtained by extrapolation from their experimental profiles inside the tube to the nozzle exit location. Thus, this practice is adopted for velocities, the total temperature at the nozzle exit is obtained by assuming an adiabatic nozzle, so that the total energy is conserved throughout the nozzle [5].

Saidi and Valipour [6], in their experimental work, examined three types of gas (oxygen–helium and air), and investigated that oxygen and air produce nearly the same cold temperature difference and that helium produces more. They related this phenomenon to their specific heat capacity ratio. Helium has more specific heat capacity ratio than oxygen and air. So, they believed that the cold temperature difference increased by increasing the specific heat capacity ratio. Stephan et al. [7] also use these three gases, and investigated that the energy separation in the vortex tube is much more effective with helium than that with air or oxygen. They also investigated that there is practically no difference in distributions of the cold gas temperature difference when air or oxygen is used as a working medium. They believed that this is due to the fact that the molecular weight of helium is much smaller than that of air or oxygen. Aydin and Baki [8] experimented with air, oxygen and nitrogen. The results obtained using nitrogen are found to lead to higher temperature differences in the vortex tube.

As we reviewed the literature, there were no numerical analyses to investigate the effects of gas type on the performance of the vortex tube. There was no comprehensive numerical work for studying the effect of vortex tube diameter; most were experiments. One [9], who undertook his work numerically, just investigated two different diameters and concluded that vortex tubes have a better performance with smaller diameters. We do not believe this is sufficient, so in the present work, 5 different diameters have been used for studying in depth.

In the present work, different gases were used as a refrigerant in a vortex tube, to understand which one produces maximum cooling temperature differences. To do this, helium,

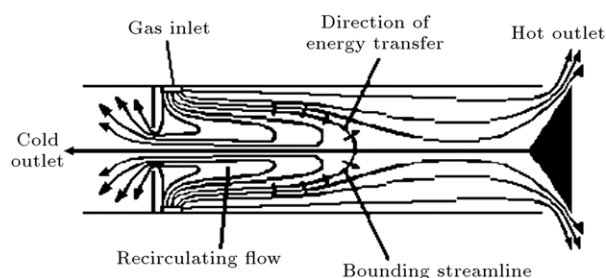


Figure 1: Schematic diagram of vortex tube (counter-flow).

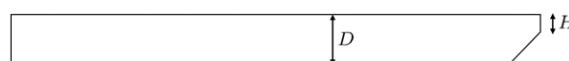


Figure 2: Vortex tube with cone shaped hot outlet.

air, nitrogen, oxygen, carbon dioxide, ammonia and water were selected. Also, the effects of varying the geometry of vortex tube components, such as hot outlet and diameter size, on tube performance, have been studied.

The hot outlet valve should be sufficiently far away from the nozzle, D (about 50 R), so that the gas reaching it will have lost most of its screw-like motion, because of internal friction. Gao [10] experimentally investigated three different types of hot end plug: spherical, plate-shaped and cone-shaped. The parameters that characterized plug type were the number of exhaust orifices, the diameter of the exhaust orifice, and the ratio of the total exhaust area and the vortex tube cross-sectional area in each type of plug. Energy separation effects were also observed in the experiments without the hot-end plug. It was concluded that the hot-end plug is not a critical component in the RHVT, due to the few differences between the results for different plugs. Aydin and Baki [8] investigated the effect of the angle of the cone-shaped control valve on the performance of a counter flow RHVT, changing the vane angle from 45° to 60° . The angle of the control valve yielding optimum performance was 50° .

Another comprehensive study was done by Markal et al. who concluded that valve angle has a weak influence on vortex tube performance [11].

In this study, different lengths of hot outlet, and, also, ones with a 45° cone shape, have been studied, as shown in Figure 2.

Different experiments and analyses have different opinions about the effects of tube diameter on the performance of vortex tubes. Some of them state that smaller vortex tubes have better performance.

Aljuwayhel et al. concluded that the reduction in energy separation with increasing diameter is directly related to the magnitude of the gradients of angular velocity. Because the same inlet boundary conditions (the inlet area, stagnation pressure, stagnation temperature, and velocity components) are used, the magnitude of gradients in angular velocity is much lower in larger diameter cases. Because angular velocity gradients give rise to tangential work transfer, the energy separation is reduced. They concluded in their article that in general, smaller diameter vortex tubes will provide more temperature separation than those with larger diameter [9]. Keyes found that tube diameter is the most important geometrical variable influencing vortex strength, as the periphery Mach number increases with a reduction in tube diameter. He reported that this improvement is due to a decrease in the turbulent wall shear, as a result of the decrease in the tangential peripheral Reynolds number. The vortex tube

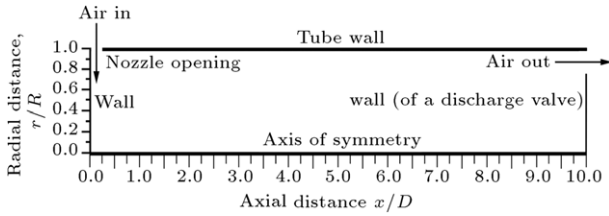


Figure 3: Computational domain of the flow system in vortex tube of Hartnett and Eckert.

diameters used in the study were 16, 25 and 50 mm [12]. A very large tube diameter would result in lower overall tangential velocities, both in the core and in the periphery region, which would produce a low diffusion of mean kinetic energy and, also, low temperature separation [3].

Some of them stated that the performance of the vortex tube is better with a larger diameter.

Hilsch concluded that smaller values of D would certainly be less favorable. If they were chosen, the rotating flow would decrease too quickly, on account of the small rate of flow and the more important contribution of friction between the gas and walls. Larger values of D would result in such large rates of flow that it could not be carried by the tube without increasing the pressure, p_i , to too large a value. This would make the expansion ratio, $\frac{p}{p_i}$, unfavorable [13].

Negam et al. stated that the vortex tube performance depends only on Reynolds number for geometrically similar tubes and under the same operating conditions. They found that a vortex tube diameter gives the maximum cold temperature drop at different inlet pressures of 16 mm. Their findings agree well with the Hilsch experiments conducted on 4.6, 9.6 and 17.6 mm tube diameters. They concluded that tube performance improves with an increase in its diameter [12]. For

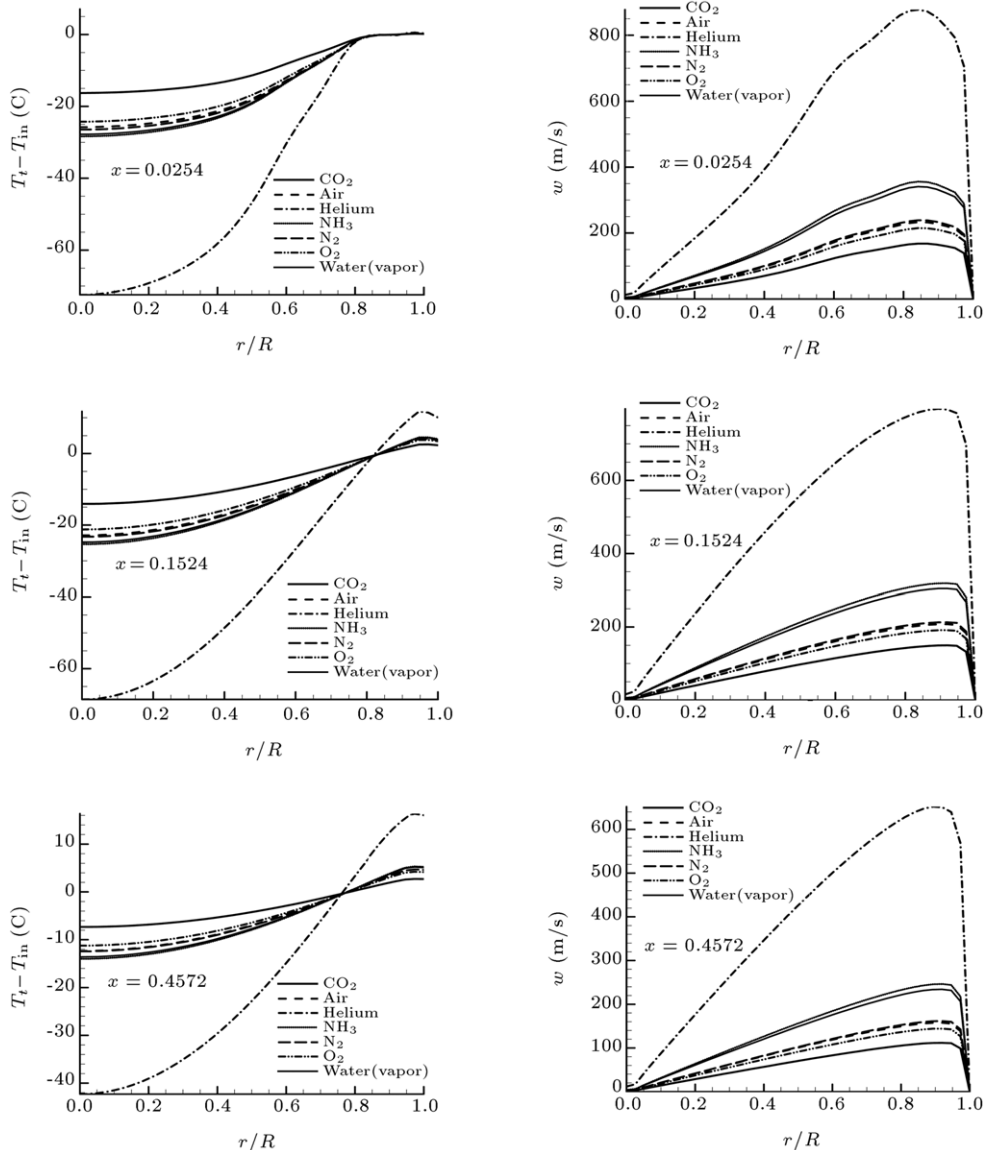


Figure 4: Radial distribution of total temperature and swirl velocity for different gases.

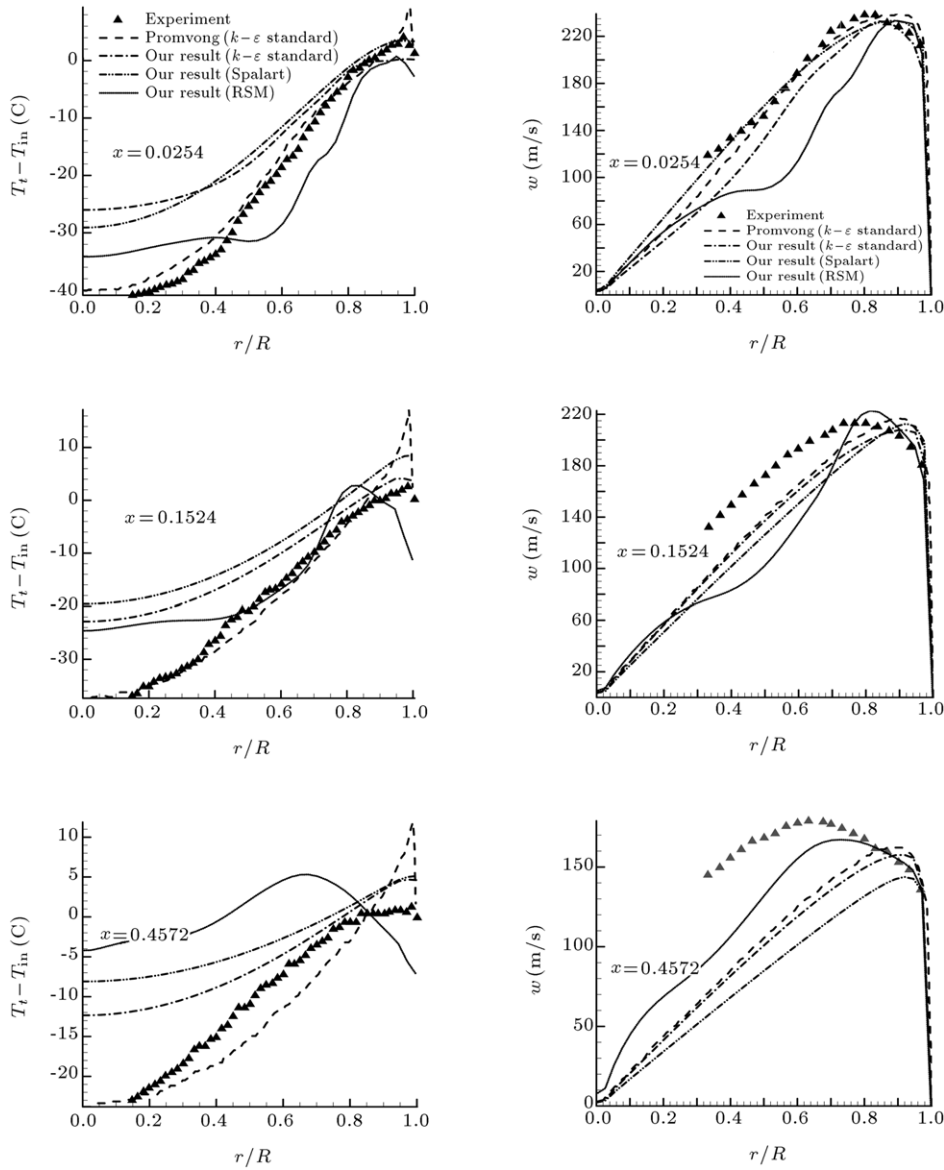


Figure 5: Radial distribution of total temperature and swirl velocity for air.

fixed inlet conditions (supply pressure) a very small diameter vortex tube would offer considerably higher back pressures, and, therefore, the tangential velocities between the periphery and the core would not differ substantially, due to the lower specific volume of air (still high density), while the axial velocities in the core region are high. This would lead to a low diffusion of kinetic energy, which also means low temperature separation [14].

The vortex tube of Hartneet and Eckert has been chosen because of the availability of experimental data with air. Moreover, when comparing our results with experimental data, we used the numerical results of Eiamsa-ard and Promvonge [14], with the k -epsilon turbulence model. The FLUENT™ software package was used to create the CFD model of the working length of the vortex tube, pictured in Figure 3. The model is two-dimensional, axisymmetric (with swirl), steady state, and employs the Standard k -epsilon and Spalart–Allmaras turbulence models. Input data values needed in the present calculation are given in [14].

2. Governing equations

The Spalart–Allmaras model is a relatively simple, one-equation model that solves a modeled transport equation for the kinematic eddy (turbulent) viscosity.

The transport equation for $\tilde{\nu}$ (The transported variable in the Spalart–Allmaras model) is:

$$\frac{\partial}{\partial t} (\rho \tilde{\nu}) + \frac{\partial}{\partial x_i} (\rho \tilde{\nu} u_i) = G_\nu + \frac{1}{\sigma_\nu} \frac{\partial}{\partial x_j} \left[(\mu + \rho \tilde{\nu}) \frac{\partial \tilde{\nu}}{\partial x_j} \right] + C_{b2} \rho \left(\frac{\partial \tilde{\nu}}{\partial x_j} \right)^2 - Y_\nu + S_{\tilde{\nu}}, \quad (3)$$

where, G_ν is the production of turbulent viscosity and Y_ν is the destruction of turbulent viscosity. σ_ν and C_{b2} are constants, ν is the molecular kinematic viscosity and $S_{\tilde{\nu}}$ is a user-defined source term.

The Standard k - ϵ model, based on the transport equations of the turbulent kinetic energy, k , and its rate of dissipation, ϵ , was

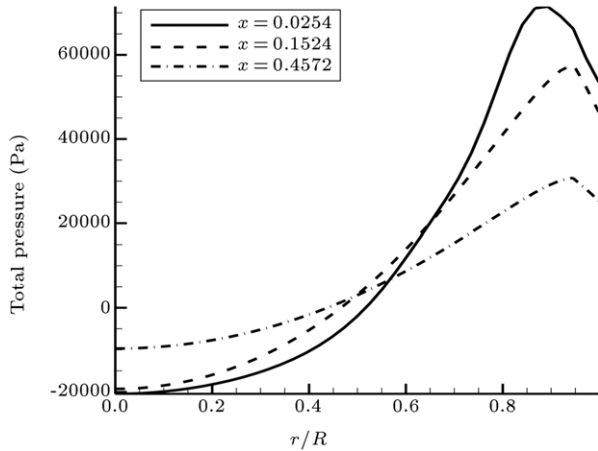


Figure 6: Radial distribution of total pressure at $x = 0.0254$, $x = 0.1524$ and $x = 0.4572$ for air.

employed to solve the vortex flow. This model is valid for fully turbulent flows that can be found in the vortex tube. Transport equations for the k - ε model are obtained as follows [15]:

$$\frac{\partial}{\partial t} (\rho k) + \frac{\partial}{\partial x_i} (\rho k u_i) = \frac{\partial}{\partial x_i} \left[\left(\mu + \frac{\mu_t}{\sigma_k} \right) \frac{\partial k}{\partial x_j} \right] + G_k + G_b - \rho \varepsilon - Y_M + S_k, \quad (4)$$

$$\frac{\partial}{\partial t} (\rho \varepsilon) + \frac{\partial}{\partial x_i} (\rho \varepsilon u_i) = \frac{\partial}{\partial x_i} \left[\left(\mu + \frac{\mu_t}{\sigma_k} \right) \frac{\partial \varepsilon}{\partial x_j} \right] + C_{1\varepsilon} \frac{\varepsilon}{k} (G_k + C_{3\varepsilon} G_b) - C_{2\varepsilon} \rho \frac{\varepsilon^2}{k} + S_\varepsilon. \quad (5)$$

G_k represents the generation of turbulent kinetic energy caused by the mean velocity gradients. This term can be calculated from $G_k = \mu_t S^2$, where S is the modulus of the mean rate-of-strain tensor. G_b is the generation of turbulent kinetic energy due to buoyancy. For an ideal gas, this term is calculated from buoyancy effects on the generation of k , which buoyancy effects are included for a non-zero gravity field and a non-zero temperature gradient. Y_M is related to the effects of compressibility on turbulence. This can be obtained from $Y_M = 2\rho\varepsilon M_t^2$, where M_t is Mach number. $C_{1\varepsilon}$, $C_{2\varepsilon}$ and $C_{3\varepsilon}$ are constants and are given at 1.44, 1.92 and 0.09, respectively. S_k and S_ε are the turbulent Prandtl numbers for k and ε , which are given at 1 and 1.3, respectively. These five values are the default, which are referred to from experiments with air for turbulent shear flows. S_k and S_ε are user-defined source terms, and μ_t is the turbulent viscosity [15].

3. Boundary condition

The inlet is modeled as a mass flow inlet; the total mass flow rate, stagnation temperature and direction vector were specified. The hot exit is represented as pressure outlet using atmosphere static pressure. A no-slip boundary condition is enforced on all walls of the vortex tube. The dynamic viscosity, generally, is a function of the temperature. However, in the present computations, it is assumed to be uniform throughout, because the temperature change in the vortex tube is not large. The computational domains of the flow system are shown in Figure 3.

There are approximately 30,000 cells. The use of a higher number of cells is shown not to make much difference to simulation results.

We have considered steady-state, axisymmetric compressible flow in the vortex tube with negligible body force and without an energy sources.

The vortex tube is well insulated from its surroundings. The gas flowing through the vortex tube is considered as an ideal gas. The governing equations, continuity, momentum and energy, are solved using the pressure-based solver of Fluent 6.3, with ideal gas assumption for air.

4. Results

The results will be introduced in this section. These include the effects of gas properties, turbulence models and geometrical parameters on the performance of a vortex tube.

4.1. Effect of gas and turbulence models

Total temperature is defined as:

$$T_t = T_s + \frac{V^2}{2c_p}. \quad (6)$$

The properties of different gases are listed in Table 1 to help evaluate the effect of specific heat capacity ratio and molecular weight on energy separation in a vortex tube.

Total temperature differences ($T_t - T_i$) and tangential velocity (w) profiles were provided at 3 axial locations, namely, $x = 0.0254$, 0.1524 and 0.4572 m (or $x/D = 0.333$, 2 and 6 , respectively), from the nozzle for different gases, and the results have been shown in Figure 4.

It can be seen that helium has the maximum energy separation, which can be attributed to its maximum value of specific heat capacity ratio and minimum molecular weight.

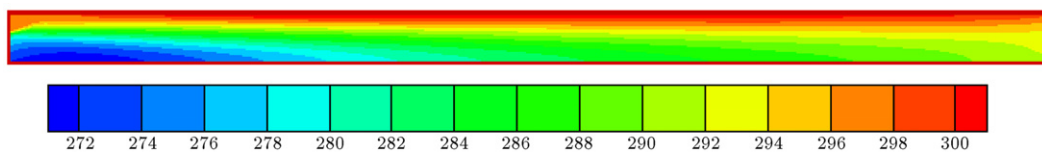


Figure 7: Contours of total temperature.

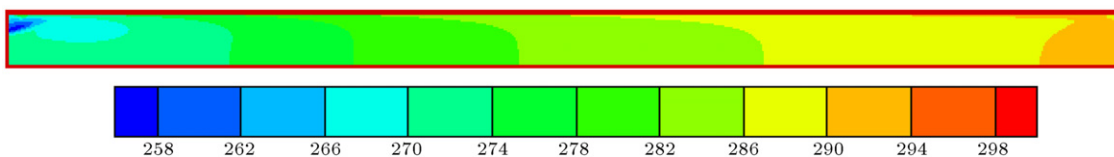


Figure 8: Contours of static temperature.

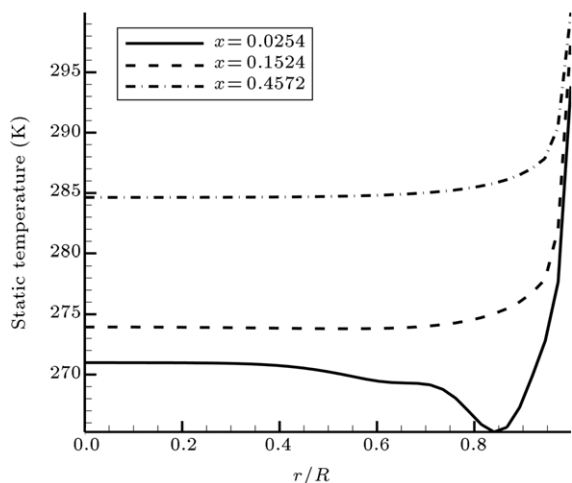


Figure 9: Variation of static temperature at $x = 0.0254$, $x = 0.1524$ and $x = 0.4572$ for standard $k-\epsilon$ model.

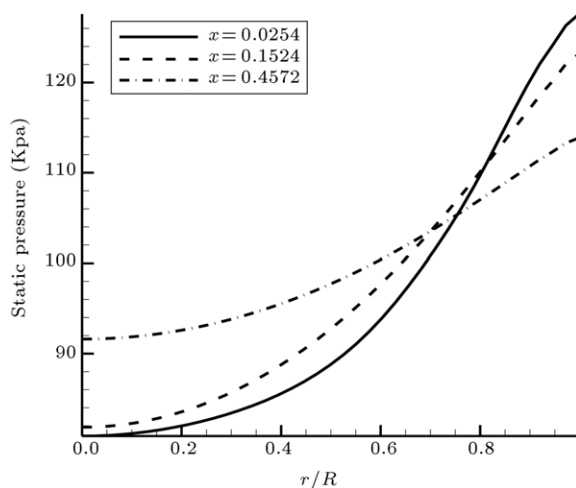


Figure 10: Radial distribution of static pressure at $x = 0.0254$, $x = 0.1524$ and $x = 0.4572$ for standard $k-\epsilon$ model.

Table 1: Properties of different gases.

Gas	Specific heat capacity ratio (k)	Molecular weight
Helium	0.1520	4.003
NH ₃	0.0247	17.031
Water (vapor)	0.0261	18.015
Nitrogen	0.0242	28.013
Air	0.0242	28.966
Oxygen	0.0246	31.999
CO ₂	0.0145	44.001

As clear from Figure 4, the cold temperature difference increases by increasing specific heat capacity ratio and decreasing molecular weight. Air and nitrogen have the same specific heat capacity ratio and molecular weight, so, they are expected to have the same energy separation, which appears true from Figure 4.

It can be seen from Figure 5 that the total temperature difference is nearly proportional to the tangential velocity magnitude. The gas in the middle region of the tube has a lower velocity and temperature than the inlet gas, and the gas near the tube wall has higher velocity and temperature than the inlet gas. The rotating air stream produces a region of increased

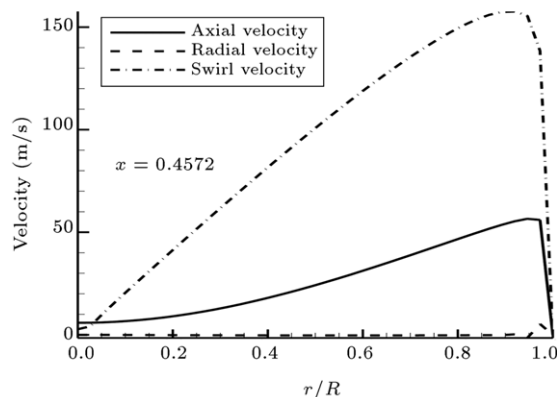
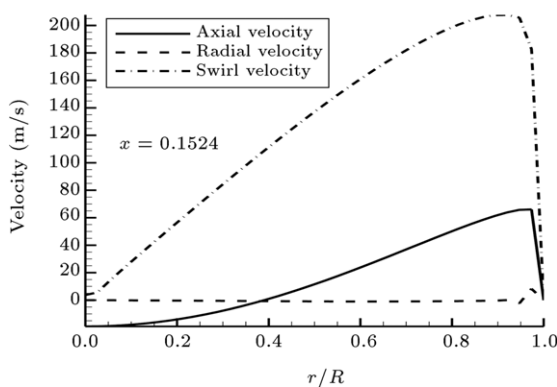
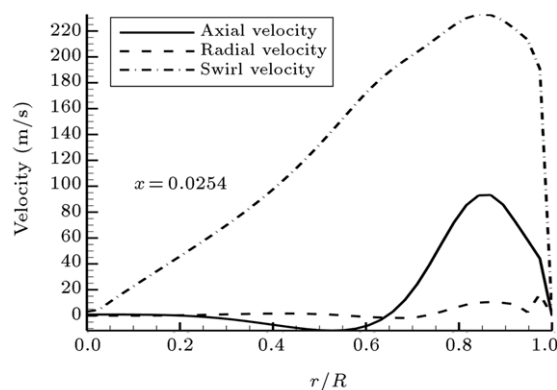


Figure 11: Radial distribution of radial, axial and swirl velocity at $x = 0.0254$, $x = 0.1524$ and $x = 0.4572$ for air.

pressure near the wall inside the cylinder, and a region of decreased pressure near the axis. The temperature separation obtained from the present calculations with air was compared with the experimental results of Hartnett and Eckert, and the computational results of Eiamsa-ard and Promvonge [14] as seen in Figure 5. Maximum relative error for velocity distribution is shown in Table 2.

Our results under-predicts the separation effect in the vortex tube. However, the shape of the curve and the qualitative trends agree very well. The radial profile of the swirl velocity indicates a free vortex near the wall, and the values become negligibly small at the core, which is in conformity with the observations of Gutsol [16].

At the tube wall, the total temperature is found to decrease. This is due to the no slip boundary condition at the tube wall.

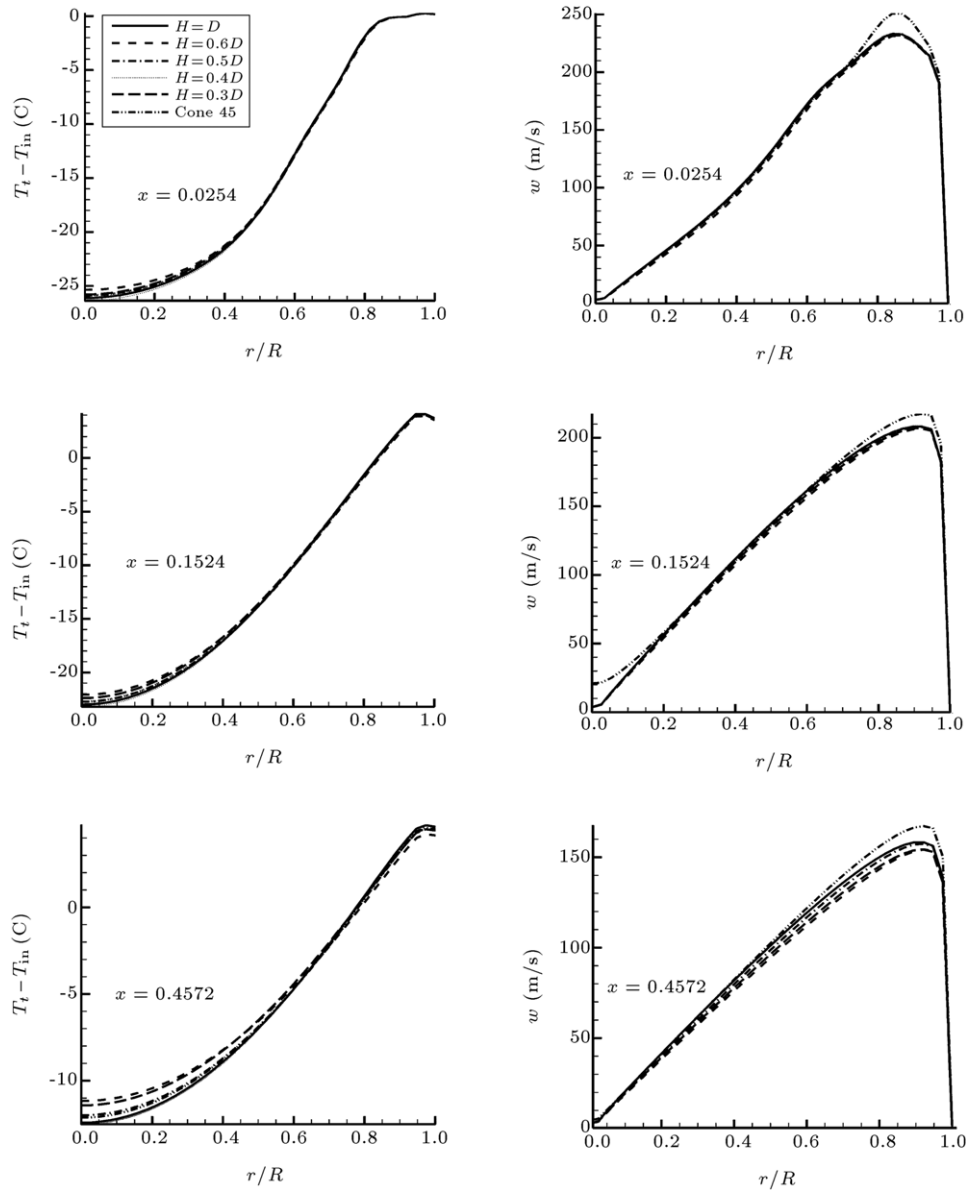


Figure 12: Effect of hot orifice on temperature separation and swirl velocity.

Table 2: Maximum relative error for velocity distribution in three axial positions.

	Promvong	Standard <i>k</i> -epsilon	Spalart-Allmaras	RSM
$x = 0.0254$	0.233333	0.333333	0.125	0.4706
$x = 0.1524$	0.280303	0.280303	0.356	0.4375
$x = 0.4572$	0.503448	0.510345	0.586	0.3793

The total pressure for the compressible fluid of constant c_p can be defined as:

$$P_0 = P_s \left(1 + \frac{\gamma - 1}{2} M^2 \right)^{\frac{\gamma}{\gamma - 1}}, \quad (7)$$

Figure 6 shows the variation of total pressure in a radial direction along the hot tube, at $x = 0.0254$, $x = 0.1524$ and $x = 0.4572$. This clearly illustrates that the flow with high

pressure is near the wall, and the flow with low pressure is in the central area, where the high inlet flow pressure is expanded, lowering the flow temperature.

Figures 7 and 8 show the contour plots of the predicted total temperature and static temperature, respectively, which are in good agreement with the results of Eiamsa-ard and Promvong [14].

It can be seen from Figures 7 and 8 that on the left hand side, between the inlet nozzle and cold outlet, the static temperature is minimum, and the static temperature of fluid exiting the cold outlet is higher than its upper. So, in this region, heat transfer occurs from the cold outlet to the nozzle, which is useful, and increases the COP of the vortex tube. But, as we proceed along the tube to the hot outlet, the static temperature near the wall become higher than the center region. This distribution reduces the performance of the vortex tube.

In Figure 9, the radial profiles of static temperature have been shown. The static temperature decreases by increasing

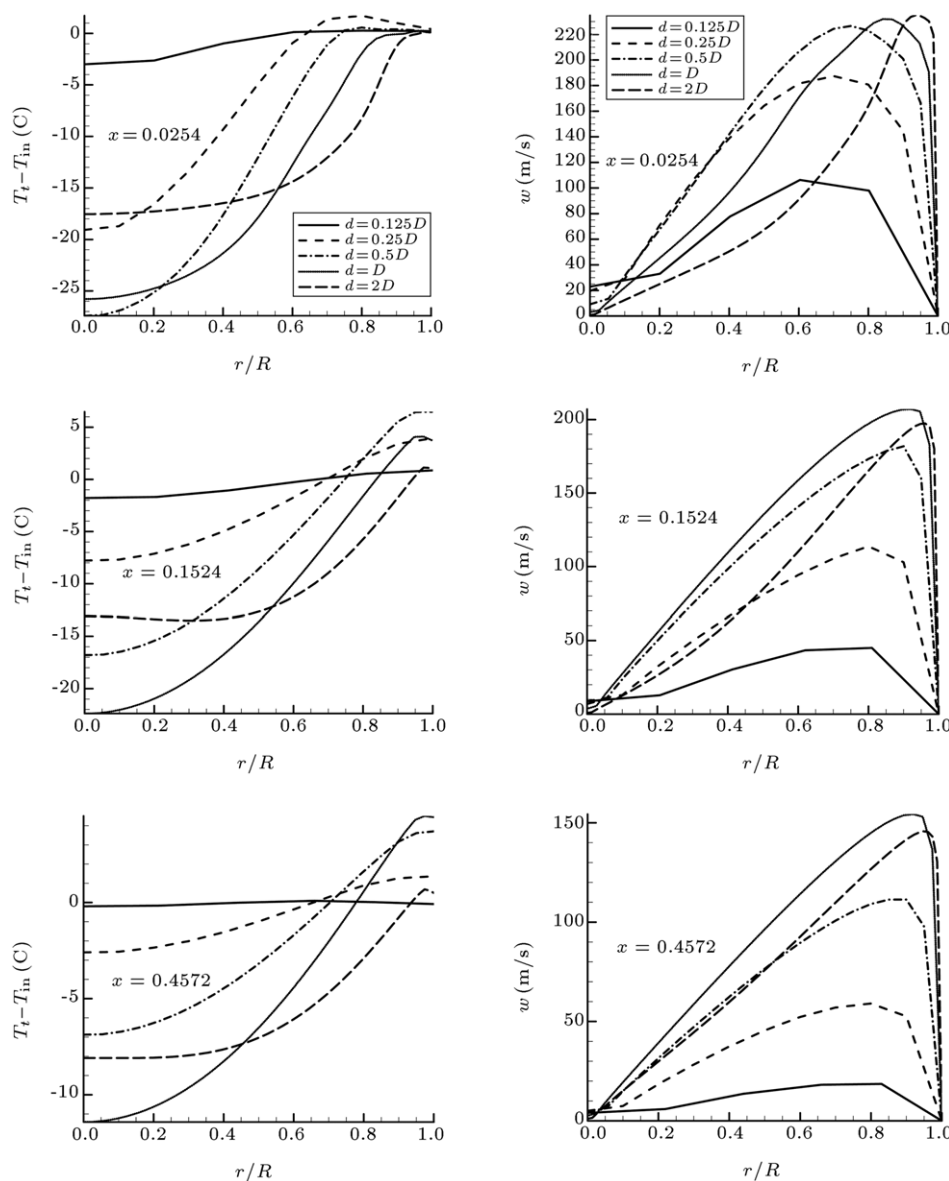


Figure 13: Radial distribution of total temperature and swirl velocity at different tube diameters.

r at $x = 0.0254$ (near the inlet nozzle). This distribution improves the performance of the vortex tube, because of the energy transfer from the cold region of the vortex tube at the axis to the hot region of the vortex tube at the periphery.

Because of centrifugal forces, fluid particles have a tendency to move towards the wall. So, the regions near the axis will have less static pressure in comparison to regions near the wall, which is shown in Figure 10. Near the wall, regions gain a considerably high temperature, as a result of the compression formed. In spite of expansion near the axis regions, a good mixing of flow always causes a homogeneous temperature in the domain. So, static temperature is supposed to be uniform in the radial direction.

It should be noted that because of the sudden velocity decrease near the wall, conduction overcomes convection, but it is vice versa near the axis regions. So, compression near the wall regions could increase temperature. But, expansion causes a uniform distribution near the axis regions. Total temperature depends on the velocity, with an order of two, and static

temperature, with an order of one. Static temperature increases near the wall, but, a significant decrease in velocity magnitude causes a decrease in total temperature near the tube walls.

4.2. Comparing radial, axial and swirl velocity

From Figure 11, it is clear that the radial velocity is significantly low in magnitude compared to axial and swirl components, and its effect can be neglected. Also, it could be concluded that swirl velocity has the most effect on the temperature separation of the vortex tube.

4.3. Effect of hot outlet

From Figure 12, it is clear that the hot outlet dimension and its shape have a negligible effect on temperature distribution in the vortex tube, which is in good agreement with work that has been done until now [2]. This behavior is a result of low swirl velocity in the hot outlet section, which is a dominant component of velocity, which causes temperature separation.

4.4. Effect of diameter

In this study, the vortex tube of Hartnett and Eckert, with different diameters, respectively, D , $2D$, $0.5D$, $0.25D$, $0.125D$, have been studied in which “ D ” is the original diameter in Hartnett and Eckert’s work. In the CFD analysis, all dimensions (except diameter), T_{in} , and velocity components for all case are the same. Total temperature differences ($T_{total} - T_{in}$) and tangential velocity (w) profiles were provided at 3 axial locations, namely, $x = 0.0254$, 0.1524 and 0.4572 m (or $x/D = 0.333$, 2 and 6 , respectively), from the nozzle, and the results have been shown in Figure 13. It can be seen that the total temperature difference is nearly proportional to the tangential velocity magnitude, and very small diameters have the worst performance, which can be attributed to low tangential velocity in the tube. At very small tube diameters of tube, the rotating flow would decrease too quickly, on account of the small rate of flow, and the more important contribution of friction between the gas and walls.

5. Conclusions

The effects of varying the geometry of vortex tube components, such as hot outlet and diameter size, on tube performance, have been studied, besides using different gases as a working medium in a vortex tube. The results showed that:

- Cold temperature difference increases by increasing the specific heat capacity ratio, and gas with lower molecular weight causes more energy separation.
- Helium was found to have the most cold temperature difference than other gases, which can be attributed to its maximum value of specific heat capacity ratio and minimum molecular weight.
- Results with air were in good agreement with experimental data and the numerical results of Promvong, with the k -epsilon turbulence model. It is concluded that total temperature difference is nearly proportional to the tangential velocity magnitude.
- It was understood that the Spalart–Allmaras turbulent model, shown in the first equation, is not so bad in predicting temperature results. Although, in most regions, the Standard k -epsilon model predicts better results.
- It is concluded that the hot outlet dimension and its shape have a negligible effect on temperature distribution in a vortex tube, because of low swirl velocity in the hot outlet.
- Very small diameters have the worst performance, which can be attributed to low tangential velocity in the tube.

Acknowledgments

The author would like to gratefully acknowledge Iman Mirzaii, Morteza Anbarsooz, Sina Alavi and Aref Afsharfard for their valuable help in preparing the presented manuscript.

References

- [1] Cockerill, T. “The Ranque–Hilsch vortex tube”, Ph.D. Thesis, Cambridge University, Engineering Department, Sunderland (1995).
- [2] Yilmaz, M., Kaya, M., Karagoz, S. and Erdogan, S. “A review on design criteria for vortex tubes”, *Journal of Heat Mass Transfer*, 45, pp. 613–632 (2009).
- [3] Eiamsa-ard, S. and Promvong, P. “Review of Ranque–Hilsch effects in vortex tubes”, *Renewable & Sustainable Energy Reviews*, (2007).
- [4] Balmer, R.T. “Pressure-driven Ranque–Hilsch temperature separation in liquids”, *Journal of Fluids Engineering*, 110, pp. 161–164 (1988).
- [5] Eiamsa-ard, S. and Promvong, P. “Numerical prediction of vortex flow and thermal separation in a subsonic vortex tube”, *Journal of Zhejiang University Science A*, 7, pp. 1406–1415 (2006).
- [6] Saidi, M.H. and Valipour, M.S. “Experimental modeling of vortex tube refrigerator”, *Applied Thermal Engineering*, 23, pp. 1971–1980 (2003).
- [7] Stephan, K., Lin, S., Dljrs, M. and Huanc, F. “A similarity relation for energy separation in a vortex tube”, *Journal of Heat Mass Transfer*, 27, pp. 911–920 (1984).
- [8] Aydin, O. and Baki, M. “An experimental study on the design parameters of a counterflow vortex tube”, *Journal of Energy*, 31, pp. 2763–2772 (2006).
- [9] Aljuwayhel, N.F., Nellis, G.F. and Klein, S.A. “Parametric and internal study of the vortex tube using a CFD model”, *International Journal of Refrigeration*, 28, pp. 442–450 (2005).
- [10] Gao, C. “Experimental study on the Ranque–Hilsch vortex tube”, Ph.D. Dissertation, Department of Applied Physics, Eindhoven University of Technology, The Netherlands (2005).
- [11] Markal, B., Aydin, O. and Avci, M. “An experimental study on the effect of the valve angle of counter-flow Ranque–Hilsch vortex tubes on thermal energy separation”, *Experimental Thermal and Fluid Science*, 34, pp. 966–971 (2010).
- [12] Negm, M., Seraj, A. and Abdull Ghani, S. “Generalized correlations for the process of energy separation in vortex tube”, *Modeling, Simulation and Control*, 14(4), pp. 47–64 (1988).
- [13] Hilsch, R. “The use of expansion of gases in a centrifugal field as a cooling process”, *Review of Scientific Instruments*, 18, pp. 108–113 (1947).
- [14] Eiamsa-ard, S. and Promvong, P. “Numerical investigation of the thermal separation in a Ranque–Hilsch vortex tube”, *Journal of Heat Mass Transfer*, 50, pp. 821–832 (2007).
- [15] Rattanongphisat, W., Riffat, S.B. and Gan, G. “Thermal separation flow characteristic in a vortex tube: CFD model”, *International Journal of Low Carbon Technologies*, pp. 282–295 (2008).
- [16] Gutsol, A.F. “The Ranque effect”, *Physics–Uspekhi*, 40, pp. 639–658 (1997).

Hossein Khazaei was born in Mashhad, Iran, in 1986. He received a B.S. degree in Fluid Mechanics from the Department of Mechanical Engineering at the Islamic Azad University of Mashhad, Iran, in 2008, and an M.S. degree in Energy Conversion from the Department of Mechanical Engineering at Ferdowsi University, Mashhad, Iran, in 2011. He has published 2 conference papers. His major fields of study are turbulence modeling and heat transfer.

Ali Reza Teymourtash received a B.S. degree in Mechanical Engineering from Ferdowsi University of Mashhad, Iran, in 1983, an M.S. degree in Mechanical Engineering (Thermofluid) from Sharif University of Technology, Tehran, Iran, in 1987, and a Ph.D. degree in Energy Conversion from Ferdowsi University of Mashhad, Iran, in 2002, where he is now Associate Professor. He has published a book in Fluid Mechanics, 25 papers in respected international conference proceedings and 12 journal papers. He has also been responsible for a number of applied industrial projects.

Majid Malek-Jafarian was born in Mashhad, Iran, in 1975. He received a B.S. degree in Fluid Mechanics from the Mechanical Engineering Department of Ferdowsi University of Mashhad, Iran, in 1997, and M.S. and Ph.D. degrees in Energy Conversion from the Mechanical Engineering Department of Ferdowsi University of Mashhad, Iran, in 1999 and 2006, respectively. His major fields of study are turbulence modeling, aerodynamics and micro flows. He is currently employed in the Mechanical Engineering Department of the University of Birjand, Iran.